LIQUID CRYSTALS, 2001, VOL. 28, NO. 9, 1315–1320

Dynamics of phase transitions in a liquid crystal probed by Raman spectroscopy

A. BHATTACHARJEE, P. R. ALAPATI† and A. L. VERMA*

Department of Physics, North Eastern Hill University, Shillong 793022, India
†Department of Physics,
North Eastern Regional Institute of Science and Technology, Itanagar 791109, India

(*Received 18 July 2000; in final form 1 November 2000; accepted 7 December 2000*)

Raman spectra of the Schiff's base liquid crystalline compound 5O5, *N*-(4-*n*-pentyloxybenzylidene)-4′-*n*-pentylaniline, have been recorded as a function of temperature from 22 to 80°C in the 1140–1220 cm^{-1} and 1550–1640 cm^{-1} spectral regions. From careful deconvolution of the spectral features using Lorentzian profiles, precise values of peak positions, integrated intensities and linewidths of some selected Raman bands were obtained. The variations of the Raman spectral parameters with temperature are discussed in terms of changes in the molecular alignment and its effect on intra-/inter-molecular interactions at the Cr–G, G–SmF, SmF–SmC and SmA–N phase transitions. From a detailed study, it is inferred that the increased orientational/vibrational freedom of the alkyl chains, as well as the delocalization of the electron clouds, is responsible for the spectral anomalies at the Cr–G transition. Loss of positional ordering and twist around the $-C_6H_4-N=$ bond takes place at the SmF–SmC transition. In the SmA–N transition, some evidence for the formation of cybotactic clusters was obtained.

1. Introduction

In recent years, Raman spectroscopy has emerged as a very useful tool in the investigation of vibrational dynamics of liquid crystalline compounds. The importance of this technique is further realized because the phase transitions in liquid crystals are reflected as variations in measurable parameters of certain vibrational modes of the system. The measurement and analysis of linewidths and peak positions yield information about the structure and dynamics of the system undergoing phase transitions. In addition, integrated intensity provides crucial information about the fluctuation of some physical quantities undergoing changes during phase transition. Extensive studies on the dynamics of phase transitions of liquid crystals using the Raman spectroscopic technique have been reported [1–11]. Most of these studies have focused attention on analysing either the region involving the lattice modes [1–6] or the 200–900 cm^{-1} region, which concerns the conformationally sensitive alkyl chain modes [7–9]. The lattice mode region is found to show some abrupt changes in intensity of certain modes with increasing temperature; these changes have been associated with the decrease in the intermolecular interactions, as well as positional ordering. Intensity changes in the alkyl chain mode region have been ascribed to the fact that at higher temperatures the increased lateral gap between the different molecular layers facilitates orientational and translational motions of the long alkyl tail along the molecular axis. However, it is necessary to monitor the behaviour of the Raman bands associated with the core and the alkyl chain parts separately, as a function of temperature and other parameters, to understand the role of these units in the dynamics of phase changes.

In this work we have carried out extensive studies of the liquid crystal 5O5 using laser Raman spectroscopy. We have investigated the behaviour of the various core-related bands as a function of temperature in the different phases. The results obtained provide evidence for the existence of a lateral dipole moment at the core. We have also obtained evidence concerning the transition between well defined three-dimensional states and also on the loss of positional ordering and twisting of the molecular segments at the $-C_6H_4-N=$ bond.

2. Experimental

The sample of 5O5 was synthesized following a procedure described elsewhere [12]. The sample was repeatedly recrystallized from absolute ethanol until the

*Author for correspondence; e-mail: alverma@dte.vsnl.net.in

Liquid Crystals ISSN 0267-8292 print/ISSN 1366-5855 online © 2001 Taylor & Francis Ltd
http://www.tandf.co.uk/journals
DOI: 10.1080/02678290110038201

observed transition temperatures were found to be constant. The transition temperatures were obtained using DSC and polarizing optical microscopy with a hot stage and found to be in excellent agreement with values reported in the literature [12–15]. For obtaining the Raman spectra, the sample was inserted in a 0.5 mm diameter quartz capillary tube in an inert atmosphere and sealed at both ends. This sealed tube was placed in an evacuated chamber inside a home-made high temperature cell. The temperature was monitored continuously and kept stable within an accuracy of ± 0.2°C with the help of a copper–constantan thermocouple placed in close contact with the sample. The Raman spectra of the sample were recorded at various temperatures on a Spex Ramalog 1403 double monochromator, equipped with an RCA-31034 photomultiplier tube and a CCD detector, in the 1140–1220 and 1550–1640 cm^{-1} regions. The spectra were recorded over a wide range of temperatures starting from 22°C (crystalline solid phase) to 76°C (isotropic liquid) at intervals of 0.3°C near phase transitions and 2°C elsewhere. The excitation source used was the 488.0 nm line from an Ar^+ laser. In order to avoid laser heating of the sample, very low laser power (20–30 mW) was employed. A scanning increment of 0.1 cm^{-1} with an integration time of 0.5 s was found suitable for recording the spectra with a reasonably good signal to noise ratio with the slit combination of 200-400-400-200 μm. Our data had a very high reproducibility with the uncertainty in the peak positions being within ± 0.20 cm^{-1}, while the band areas and linewidth (FWHM) were accurate within ± 2%. A few spectra at low temperature (30 K) were also recorded to ascertain the number of overlapping bands in the broad spectral regions. The spectra obtained were deconvoluted and the various spectral parameters were calculated using the GRAMS software.

3. Results and discussion

3.1. *Molecular structure*

The structure and phase transition sequence of *N*-(4-*n*-pentyloxybenzylidene)-4′-*n*-pentylaniline (abbreviated as 5O5) are shown below (figure 1):

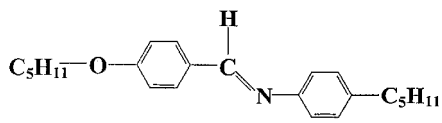

Cn $\overset{28\,^{\circ}C}{\rightleftharpoons}$ G $\overset{47\,^{\circ}C}{\rightleftharpoons}$ SmF $\overset{49\,^{\circ}C}{\rightleftharpoons}$ SmC $\overset{53.1\,^{\circ}C}{\rightleftharpoons}$ SmA $\overset{54.4\,^{\circ}C}{\rightleftharpoons}$ N $\overset{77.8\,^{\circ}C}{\rightleftharpoons}$ I

Figure 1. Structure and phase transition sequence of liquid crystalline compound 5O5, *N*-(4-*n*-pentyloxybenzylidene)-4′-*n*-pentylaniline.

The molecule is composed of two portions, the two benzene rings with the −C(H)=N− linkage forming the core; and the C_5H_{11} alkyl chains forming the zig-zag tails, which are attached to the two ends of the core. The Raman spectrum showed a triplet in the 1160–1171 cm^{-1} region (figure 2). Similarly, doublets were observed in the 1570–1575 and 1594–1598 cm^{-1} regions (figure 2). The occurrence of the triplets and doublets can be attributed to the presence of the oxygen atom. A question is likely to arise here as to whether the origin of the triplet and the doublets is due to the delocalization of the charges or to the presence of different rotational isomers. The possibility of the occurrence of rotational isomers can be eliminated for two main reasons. The splittings in the triplet, and doublets became much clearer in the Raman spectrum at low temperatures (≈ 30 K). If rotational isomers were present, we would have expected at least a reduction in the splitting, if not the complete replacement of the doublets by singlets. Another important piece of evidence is obtained from a close look at the spectrum. At low temperatures and also up to a temperature of 51°C, the band at 1167 cm^{-1} is more intense than the band at 1162 cm^{-1}, whereas at higher temperatures the relative intensity of these bands changes. Such an effect would not be observed in the case of rotational isomers, as the intensity of Raman bands is a function of the population of the two forms. The band at 1171 cm^{-1} is assigned to the C−O stretching mode of the molecule. The bands observed at 1162 and 1167 cm^{-1} are the in-plane C−H bending modes of the two aromatic rings. Similarly the bands arising at 1572, 1575, 1594 and 1598 cm^{-1} are due to the quadrant stretching modes of the aromatic rings [10, 16]. The oxygen atom adjacent to one of the aromatic rings strongly affects the band positions. The electronegativity of oxygen (3.5) is higher than that of carbon (2.5); for this reason, a large change in the electron cloud distribution takes place, resulting in the development of a slight negative charge at the oxygen atom with respect to the aromatic ring. On the other hand, there is a nitrogen atom attached to the second aromatic ring; this will disturb the electron cloud distribution of this aromatic ring, but not to the same extent as the oxygen atom, as the difference in electronegativity in this case is somewhat lower (electronegativity of N = 3). To explore this aspect in detail, we consider the electronic configuration of oxygen:

$$(1s_{\sigma}^{b})^2(1s_{\sigma}^{a})^2(2s_{\sigma}^{b})^2(2s_{\sigma}^{a})^2(2p_{\sigma}^{b})^2(2p_{\pi}^{b})^4(2p_{\pi}^{a})^2$$

where b and a stand for bonding and anti-bonding orbitals, respectively. The delocalization of the π-electrons takes place due to the mesomeric effect [16]. In such a case, a lateral dipole develops along the central linkage [17]. Such a dipole would have a tendency to reduce

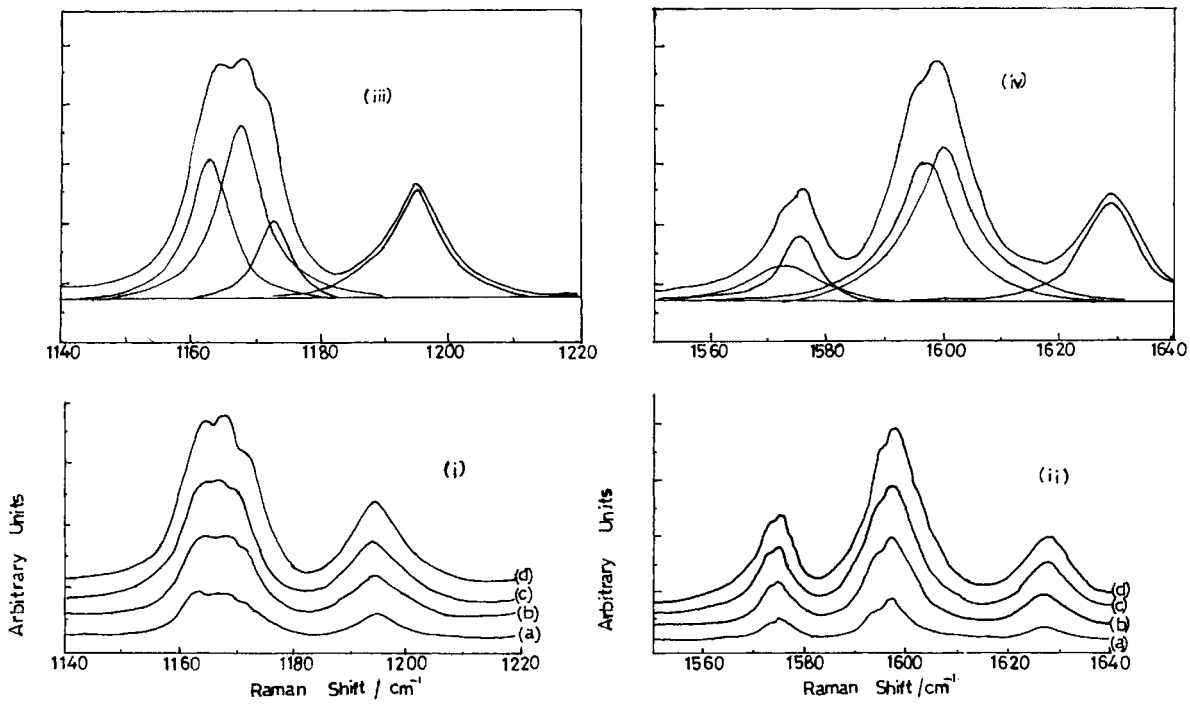

Figure 2. Raman spectra in the 1140–1220 cm^{-1} (i) and 1550–1640 cm^{-1} (ii) regions for different phases. (a) Crystalline phase, (b) G phase, (c) smectic C phase, (d) smectic A phase. Panels (iii) and (iv) show the deconvoluted spectra in the respective regions in the Smectic A phase—from spectra (d).

the extent of positional correlation of the molecules, and this is actually observed in our experiments. We can thus conclude that the charge redistributions of the two aromatic rings are different and independent of each other to a large extent. This suggests that the bands at 1162, 1572 and 1594 cm^{-1} are associated with the benzene ring adjoining the nitrogen atom and those at 1167, 1575 and 1598 cm^{-1} with the benzene ring adjacent to the oxygen atom. This is supported by the fact that we have obtained doublets for each of the aromatic ring modes instead of singlets. Further support for this view is provided by previous experiments on similar Schiff's bases without the oxygen atom (e.g. TBBA, TBDA, etc.) [10] where only singlets are observed for these particular modes of the aromatic rings. In the table, a tentative assignment of all the peak positions has been made on the basis of the expected group frequencies and reported assignments for similar Schiff's bases [10, 11, 16].

Table. Assignment of the various core-related modes of the 5O5 molecule.

Serial no.	Band position cm^{-1}	Assignment
1	1162	Aromatic C–H in plane bending mode
2	1167	Aromatic C–H in plane bending mode
3	1171	C–O stretch
4	1194	Aromatic C–N stretching mode
5	1572	Quadrant stretching mode of the aromatic ring
6	1575	Quadrant stretching mode of the aromatic ring
7	1594	Quadrant stretching mode of the aromatic ring
8	1598	Quadrant stretching mode of the aromatic ring
9	1627	C=N stretching mode

3.2. *The Cr–G phase transition*

For a detailed analysis, the bands were deconvoluted by fitting the spectral features in the 1140–1220 and 1550–1640 cm^{-1} regions (figure 2) into Lorentzian profiles at every temperature. The values of the peak positions, linewidths and integrated intensities thus obtained are plotted in figures 3, 4 and 5, respectively. The percentage contribution of individual bands to their respective overlapping spectral regions was calculated and taken as a measure of the integrated intensity. Measurement of the integrated intensity with respect to some internal standard is avoided because doping may change the characteristics of the sample. In this study we have concentrated on the structural disorder of the core and therefore we consider only the nine prominent Raman bands observed at 1162, 1167, 1171, 1194, 1572, 1575, 1594, 1598 and 1627 cm^{-1}, which are all associated with the core.

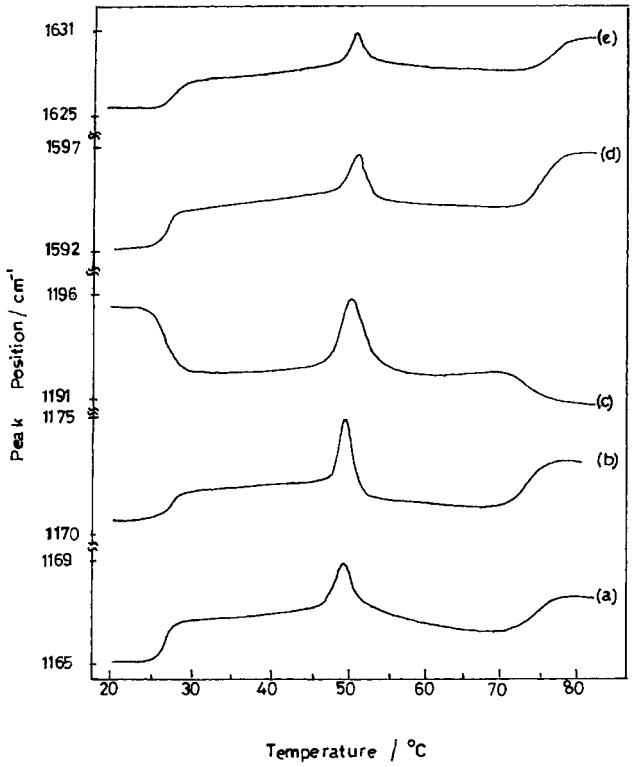

Figure 3. Variation of peak positions of the individual bands as a function of temperature. (a) 1167 cm^{-1}, (b) 1171 cm^{-1}, (c) 1194 cm^{-1}, (d) 1594 cm^{-1}, (e) 1627 cm^{-1} (uncertainty within $\pm 0.2\,cm^{-1}$).

A careful examination of these figures reveals an anomalous behaviour of the spectral features for all the Raman bands at 28°C, which is the Cr–G transition temperature for 5O5. This transition is an example of a transition between two well defined three-dimensional structures [18, 19]. The difference between the two phases is that the G phase is a highly viscous, soft crystalline phase, where the molecules are arranged in a monoclinic lattice, whereas Cr is a true crystalline solid. As for most mesogenic molecules, the alkyl chain part of the molecule is expected to attain a higher degree of orientational and vibrational freedom at the melting process involving a phase transition from a crystalline to a soft crystalline phase. In contrast, the core part of the molecule, including the aromatic rings, is expected to be rigid with very little orientational freedom. Moreover, the G phase has a pseudo-hexagonal packing with a local herring-bone structure. In such a packing order, very little translational freedom between the molecules is allowed. However, one should also remember that the lateral gap which exists among each of the pseudo-hexagonal clusters may enable the alkyl chains to move freely, thereby putting some strain on the core. For this reason, abnormalities are expected to arise in those Raman modes which are connected to the core.

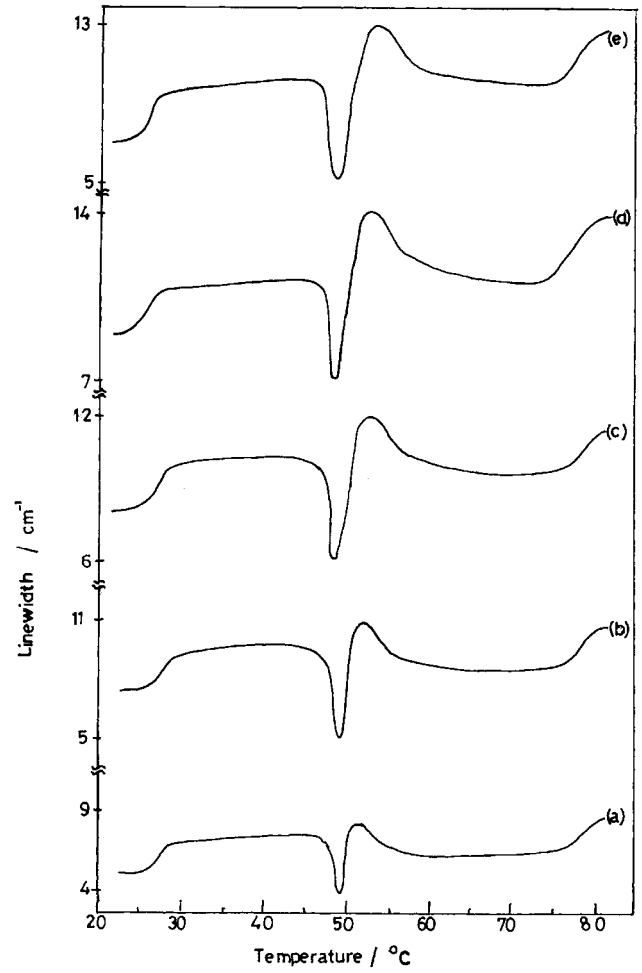

Figure 4. Variation of linewidths of the individual bands as a function of temperature. (a) 1167 cm^{-1}, (b) 1171 cm^{-1}, (c) 1194 cm^{-1}, (d) 1594 cm^{-1}, (e) 1627 cm^{-1} (uncertainty within $\pm 2\%$).

A careful study of figure 3 shows that the peak position of the Raman bands at 1167, 1171, 1594 and 1627 cm^{-1} at the Cr–G transition show a shift towards the higher side. However, the band due to the $-C_6H_4-N=$ stretching mode at 1194 cm^{-1} shows an opposite behaviour and the peak position is shifted to a lower wave number. This happens because the increased orientational freedom of the terminal alkyl chains in the G phase exerts strain on the core and softens the $-C_6H_4-N=$ bond. The Raman bands due to the C=N and the C–O modes show no appreciable shift in the peak positions because the total energy of the bonds remains unchanged. For the aromatic ring modes, the abnormality observed in the upward shift in the peak position indicates that the aromatic rings in the solid state are constrained in a stressed position due to higher interactions in the close packing.

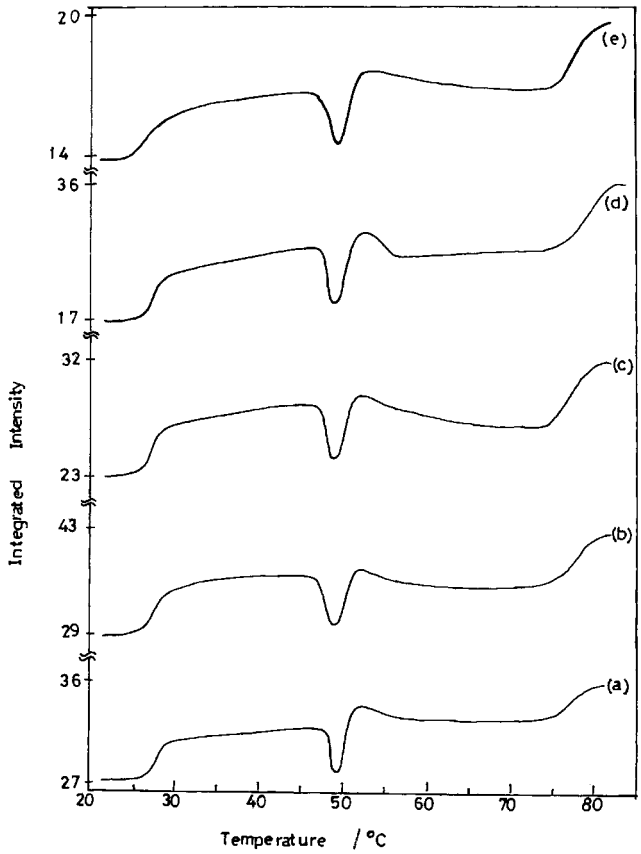

Figure 5. Variation of integrated intensities of the individual bands as a function of temperature. (a) 1167 cm^{-1}, (b) 1171 cm^{-1}, (c) 1194 cm^{-1}, (d) 1594 cm^{-1}, (e) 1627 cm^{-1} (uncertainty within $\pm 2\%$).

Figure 5 exhibits an abrupt increase in the integrated intensity at the Cr–G transition for all the representative modes; this can be attributed to the increase in the electron cloud density related to these bands. As the two lone pair electrons lie in bonding orbitals, it is possible that the 5O5 molecule shows a twist along one of the single bonds, probably the $-C_6H_4-O-$ bond at the Cr–G transition. In that case a drift of the electron cloud is expected to take place. Also, in the molecular orbital approach [20], the magnitude of the resonance and hence the strength of a covalent bond is approximately proportional to the amount of overlap of the atomic orbitals of the electrons constituting the bond. In such a case we expect the core-related modes in our molecule to show an increase in intensity and also to shift to a higher position. This is exactly what is observed in the spectra obtained, where there is an upward shift in the peak positions along with an increase in the integrated intensity of the related modes in the Cr phase. Due to this disturbance of the charge density, a broadening of the linewidth also takes place, which is evident in figure 4.

3.3. *The G–SmF transition*

As is apparent from figures 3, 4 and 5, there is a gradual increase in the peak positions, integrated intensities and linewidths with increasing temperature from 30 to 47°C. No change in the peak positions, linewidths and integrated intensities of any of the bands is observed at the G–SmF transition temperature. A close look at the structures of the G and SmF phases reveals that basically both have a *c*-centred monoclinic lattice [18, 19]. The differences in these structures lie in the fact that in the SmF phase there is only short range in-plane positional correlation of the molecules, and no interlayer positional correlation as found in the G phase. The gradual increase in the peak positions and the linewidths of all the Raman modes indicates higher freedom of the individual molecules in the SmF phase. However, the integrated intensity shows no significant change in this region. This can be understood by the fact that in this transition, the only change is the loss of intermolecular ordering, with almost no change in the intermolecular parameters either with respect to position or orientation.

3.4. *The SmF–SmC transition*

The SmF–SmC transition is marked by a sharp increase in the peak positions, whereas there is a sharp decrease in the linewidths and the integrated intensities, confirming the first order nature of this transition. This behaviour is due to the large structural differences between the SmF and SmC phases. The SmF–SmC transition is between the more ordered SmF phase and the liquid-like layers of the SmC phase. The SmF phase is characterized by a monoclinic lattice structure with hexagonal close packed molecules and short range positional ordering (bond orientational order) [18, 19]. Accordingly, the direction of the tilt is towards the edges of the hexagons. The SmC phase with its liquid-like two-dimensional structure possesses only short range correlation between the molecular positions (centres of masses) over certain distances (known as clusters). Because of the fluid-like character, neither is the distance between the centres of clusters related to the local spacing nor are the intermolecular interactions correlated.

As the intermolecular interactions are weak in the SmC phase, intramolecular dynamics are the reason behind the changes in the Raman parameters of the different modes. Therefore in the SmC phase there is a higher degree of both positional and orientational freedom of the molecules. Due to the freedom enjoyed by the molecules in this state, the bonds become stronger, and also twisting around single bonds becomes possible.

Figure 3 exhibits a small but noticeable change in the peak positions at this transition. On the other hand, the changes in the integrated intensity and linewidth

are much sharper (figures 4 and 5), especially for the $-C_6H_4-N=$ and the $-CH=N-$ modes. It is known that the Raman linewidth is a cumulative effect of the linewidths originating from the temperature-dependent reorientational motion and the temperature-independent vibrational dephasing [10 *b*]. Therefore there must be some rotational motion occurring around the $-C_6H_4-N=$ bond. The abrupt change in integrated intensity of the bands due to the $-C_6H_4-N=$ mode indicates an appreciable σ-electron cloud distortion due to rotation about this bond. In such a case, we also expect a redistribution of the π-electron cloud over the $-CH=N-$ bond, which is actually observed as a change in integrated intensity. Also, a rotation about the $-C_6H_4-N=$ bond would lead to a modification of the core of the molecule. Because of the higher freedom and comparatively weak intermolecular interactions in the SmC phase, the alkyl chains in this phase will try to stabilize themselves in the lowest energy conformation by reorienting the peripheral benzene rings around a flexible single bond ($-C_6H_4-N=$) without affecting their backbones significantly.

3.5. *The SmA–N transition*

A gradual change in the peak positions, integrated intensities and linewidths for all the bands was observed at the SmA–N transition, indicating its second order nature. However, the increase in integrated intensity for all the bands at this transition indicates that the restrictions on the molecules disappear along with the disappearance of the one-dimensional density wave characterizing the layered structure of the SmA phase along the director. This leads to a more liquid-like nematic phase with retention of a small degree of orientational order. It has been reported that the SmA–N transition in 5O5 is a second order transition with large pretransitional effects, predominantly on the nematic side; this is based upon density, ultrasonic velocity and X-ray diffraction studies [13, 14, 15]. The formation of cybotactic clusters in the nematic phase just above the SmA–N transition explains the pretransitional effects. Also the smectic-like ordering (cybotactic clusters) in the nematic phase itself may be the reason for second order nature of the SmA–N transition. Accordingly, in our present results a noticeable change is observed only in the integrated intensity of all the peaks at the SmA–N transition which may be attributed to the total disappearance of positional ordering. No changes are observed in the peak positions and the linewidths, indicating that there is no change in the molecular configuration at the transition and that the orientational order among the molecules is still retained in the nematic phase.

3.6. *The N–I transition*

The N–I transition is marked by a rather large two phase coexistence region (about 2°C) as is evident from the irregular behaviour observed in the peak positions, integrated intensities and linewidths of all the bands monitored.

The authors gratefully acknowledge financial support from the Department of Science and Technology, New Delhi.

References

[1] Bulkin, B. J., and Prochaska, F. T., 1971, *J. Chem. Phys*., **54,** 635.
[2] Borer, W. J., Mitra, S. S., and Brown, C. W., 1971, *Phys. Rev. Lett*., **27,** 379.
[3] Fontana, M., and Bini, S., 1976, *Phys. Rev. A*, **14,** 1555.
[4] Amer, N. M., and Shen, Y. R., 1973, *Solid State Commun*., **12,** 263.
[5] Amer, N. M., Shen, Y. R., and Rosen, H., 1970, *Phys. Rev. Lett*., **24,** 718.
[6] Dvorjetski, D., Volterra, V., and Wiener-Avnear, E., 1975, *Phys. Rev. A*, **12,** 681.
[7] Amer, N. M., and Shen, Y. R., 1972, *J. Chem. Phys*., **56,** 2654..
[8] Schnur, J. M., 1972, *Phys. Rev. Lett*., **29,** 1141.
[9] Amer, N. M., and Shen, Y. R., 1972, *J. Chem. Phys*., **56,** 2654.
[10] (*a*) Dash, S. K., Singh, R. K., Alapati, P. R., and Verma, A. L., 1977, *Mol. Cryst. Liq. Cryst*., **319,** 147; (*b*) Dash, S. K., Singh, R. K., Alapati, P. R., and Verma, A. L., 1997, *J. Phys. Condensed Matter*, **9,** 7809; (*c*) Dash, S. K., Singh, R. K., Alapati, P. R., and Verma, A. L., 1998, *Liq. Cryst*., **25,** 459.
[11] (*a*) Dash, S. K., Singh, R. K., Asthana, B. P., Alapati, P. R., and Verma, A. L., 1999, *J. Raman. Specstrosc*., **7,** 302; (*b*) Dash, S. K., Singh, R. K., Alapati, P. R., and Verma, A. L., 1999, *Liq. Cryst*., **26,** 1479.
[12] Rao, N. V. S., and Pisipati, V. G. K. M., 1983, *J. Phys. Chem*., **87,** 899.
[13] Alapati, P. R., Pisipati, D. M., Rao, N. V. S., Pisipati, V. G. K. M., Paranjpe, A. S., and Rao, U. R. K., 1988, *Liq. Cryst*., **3,** 1461.
[14] Pisipati, V. G. K. M., Rao, N. V. S., Pisipati, D. M., Alapati, P. R., and Rao, P. B., 1989, *Liq. Cryst*., **167,** 167.
[15] Alapati, P. R., Pisipati, D. M., Rao, P. B., Rao, N. V. S., Pisipati, V. G. K. M., and Paranjpe, A. S., 1989, *Liq. Cryst*., **5,** 545.
[16] Colthup, N. B., Daly, L. H., and Wiberley, S. E., 1975, *Introduction to Infrared and Raman Spectroscopy* (New York: Academic Press), Chap. 4 and 8.
[17] Gray, G. W., and Goodby, J. W., 1984, *Smectic Liquid Crystals* (London: Leonard Hill).
[18] Priestley, E. B., Wojtowicz, P. J., and Sheng, P., 1975, *Introduction to Liquid Crystals* (London: Plenum Press).
[19] De Gennes, P. G., 1974, *The Physics of Liquid Crystals* (London: Oxford University Press).
[20] Hergberg, G., 1945, *Infrared and Raman Spectra of Polyatomic Molecules*, Vol. 2 (New York: Van Nostrand Reinhold Co).